

Numerical evidence of renormalons in four dimensional gauge theories

Antonio Pineda

⁽¹⁾Institut de Física d'Altes Energies (IFAE), The Barcelona Institute of Science and Technology, Campus UAB, 08193 Bellaterra (Barcelona), Spain

⁽²⁾Grup de Física Teòrica, Dept. Física, Universitat Autònoma de Barcelona, E-08193 Bellaterra, Barcelona, Spain

E-mail: pineda@ifae.es

Abstract. In this talk, we briefly review work which led to the numerical demonstration of the existence of renormalons in four dimensional gauge theories with marginal operators.

1. INTRODUCTION

The perturbative weak coupling expansions of quantum field theories are expected to be asymptotic [1]. Usually, the asymptotic behavior is identified using semiclassical methods such as instantons. Asymptotically free theories with marginal operators constitute a special case. Examples of such theories are four-dimensional non-Abelian gauge theories or the two-dimensional $O(N)$ model. For these, the structure of the operator product expansion (OPE) is believed to give rise to a specific pattern of asymptotic divergence known as (infrared) renormalon [2, 3] that cannot be obtained using standard semiclassical methods. In the two-dimensional $O(N)$ model, renormalon effects were found in the large N expansion in an explicit calculation [4], albeit suppressed by factors of $1/N$. For four-dimensional non-Abelian gauge theories no such proof exists. On the contrary, the possibility that the renormalon either does not exist or is very small was raised, see e.g. [5, 6].

Using Numerical Stochastic Perturbation Theory (NSPT) (see for instance [7, 8, 9]), the static self-energy of $SU(3)$ gauge theory was computed up to order α^{20} in [10, 11, 12]. Simulations on a large set of different lattice volumes allow for a careful treatment of finite size effects. The resulting infinite volume perturbative series of the static self-energy is in remarkable agreement with the predicted asymptotic behaviour of high-order expansions, namely with a factorial growth of perturbative coefficients known as renormalon. The motivation for this computation is that this renormalon corresponds to the leading infrared renormalon of the heavy quark pole mass: m_{OS} . Its relation to the $\overline{\text{MS}}$ mass reads

$$m_{\text{OS}} = m_{\overline{\text{MS}}} + \sum_{n=0}^{\infty} r_n \alpha_s^{n+1},$$

and the renormalon (OPE) analysis predicts $r_n \sim n!$ in a very particular way. For example, the mass of a B meson fulfills the following expansion in powers of the heavy quark mass (and



Content from this work may be used under the terms of the [Creative Commons Attribution 3.0 licence](#). Any further distribution of this work must maintain attribution to the author(s) and the title of the work, journal citation and DOI.

similarly for its analog in the adjoint representation):

$$M_B = m_{\text{OS}} + \bar{\Lambda}_B + \mathcal{O}(1/m_{\text{OS}}) , \quad m_{\tilde{G}} = m_{\tilde{g},\text{OS}} + \Lambda_H + \mathcal{O}(1/m_{\tilde{g},\text{OS}}) .$$

M_B is renormalon free. Therefore, the perturbative series

$$m_{\text{OS}} = m_{\overline{\text{MS}}} + r_0 \alpha_s + r_1 \alpha_s^2 + \dots$$

suffers from a renormalon ($r_n \sim n!$) that produces a ambiguity in the way one can sum the perturbative series, which mixes with $\bar{\Lambda}_B$. In other words

$$\delta_{np}^{(\text{pert.})} m_{\text{OS}} = \delta_{np}^{(\text{pert.})} (m_{\overline{\text{MS}}} + r_0 \alpha_s + r_1 \alpha_s^2 + \dots) \sim \Lambda_{\text{QCD}} . \quad (1)$$

This behavior can be studied in the Borel plane:

$$m_{\text{OS}} = m_{\overline{\text{MS}}} + \int_0^\infty dt e^{-t/\alpha_s} B[m_{\text{OS}}](t) , \quad B[m_{\text{OS}}](t) \equiv \sum_{n=0}^\infty r_n \frac{t^n}{n!} . \quad (2)$$

The behavior of the perturbative expansion at large orders is dictated by the closest singularity to the origin of its Borel transform ($u = \frac{\beta_0 t}{4\pi}$). It has the following form:

$$B[m_{\text{OS}}](t) = N_m \nu \frac{1}{(1-2u)^{1+b}} \left(1 + c_1(1-2u) + c_2(1-2u)^2 + \dots \right) + (\text{analytic term})$$

(where the next renormalon is located at $u = 1$), producing the following asymptotic behavior of r_n [13, 3, 14]:

$$r_n \xrightarrow{n \rightarrow \infty} N_m \nu \left(\frac{\beta_0}{2\pi} \right)^n \frac{\Gamma(n+1+b)}{\Gamma(1+b)} \left(1 + \frac{b}{(n+b)} c_1 + \frac{b(b-1)}{(n+b)(n+b-1)} c_2 + \dots \right) .$$

$$b = \frac{\beta_1}{2\beta_0^2} , \quad c_1 = \frac{1}{4b\beta_0^3} \left(\frac{\beta_1^2}{\beta_0} - \beta_2 \right) , \quad \dots$$

Over the years a lot of evidence in favour of the existence of the renormalon accumulated from heavy quark physics. Two examples that we specially like:

- Static potential: $2m + V_s$ is renormalon free. For details see [14], for instance.
- The other is to visualize how the ν -dependent logarithms that appear in perturbative computations effectively become power-like:

$$r_n \xrightarrow{n \rightarrow \infty} m_{\overline{\text{MS}}} \left(\frac{\beta_0}{2\pi} \right)^n n! N_m \sum_{s=0}^n \frac{\ln^s [\nu/m_{\overline{\text{MS}}}] }{s!} \sim \nu .$$

This can be beautifully observed in Fig. 1.

Yet, these observations are based on few orders in perturbation theory ($\sim 3, 4$), where the renormalon behavior was only starting to appear. We would like to have a proof (at the same level of existing proofs of a linear potential at long distances), beyond any reasonable doubt, of the existence of the renormalon in QCD. This is what was achieved in [10, 11, 12], which we next briefly review.

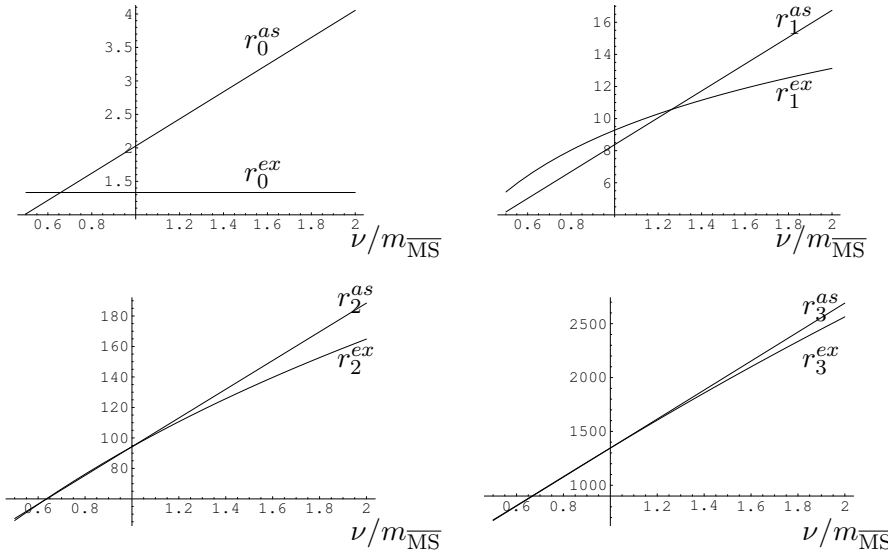


Figure 1. Plots of the exact (r_n^{ex}) and asymptotic (r_n^{as}) value of $r_n(\nu)$ at different orders in perturbation theory as a function of $\nu/m_{\overline{MS}}$. From [15].

2. POLYAKOV LOOP versus δm (and m_{OS})

The Polyakov loop on a lattice with N_T sites in the temporal direction and N_S sites in the space directions reads

$$L^{(R)}(N_S, N_T) = \frac{1}{N_S^3} \sum_{\mathbf{n}} \frac{1}{d_R} \text{tr} \left[\prod_{n_4=0}^{N_T-1} U_4^R(n) \right] = e^{-a N_T P^{(R,\rho)}(N_S, N_T)}, \quad U_\mu^R(n) \approx e^{i A_\mu^R(n+1/2)a}.$$

We implement triplet and octet representations R ($d_R = 3, 8$).

$$P^{(R,\rho)}(N_S, N_T) = \sum_{n=0}^{\infty} c_n^{(R,\rho)}(N_S, N_T) \alpha^{n+1}, \quad (3)$$

$$\delta m = \lim_{N_S, N_T \rightarrow \infty} P^{(3,\rho)}(N_S, N_T), \quad \delta m_{\tilde{g}} = \lim_{N_S, N_T \rightarrow \infty} P^{(8,\rho)}(N_S, N_T), \quad (4)$$

$$c_n^{(R,\rho)} = \lim_{N_S, N_T \rightarrow \infty} c_n^{(R,\rho)}(N_S, N_T). \quad (5)$$

$$\delta m = \frac{1}{a} \sum_{n=0}^{\infty} c_n^{(3,\rho)} \alpha^{n+1} (1/a) \text{ (fundamental)}, \quad \delta m_{\tilde{g}} = \frac{1}{a} \sum_{n=0}^{\infty} c_n^{(8,\rho)} \alpha^{n+1} (1/a) \text{ (adjoint)}.$$

δm and $\delta m_{\tilde{g}}$ are the energies of static colour sources in the fundamental and adjoint representation, respectively. δm shares the same infrared behavior as the pole mass. Therefore, we have

$$\lim_{n \rightarrow \infty} c_n^{(3,\rho)} = r_n(\nu)/\nu.$$

2.1. Perturbative OPE at finite volume

We then have to obtain the $(N_T, N_S) \rightarrow \infty$ limit of these coefficients. The N_T dependence is weak. We then focus on the N_S dependence.

$$\delta m(N_S) \equiv \lim_{N_T \rightarrow \infty} P(N_S, N_T) \quad \text{and} \quad c_n(N_S) \equiv \lim_{N_T \rightarrow \infty} c_n(N_S, N_T).$$

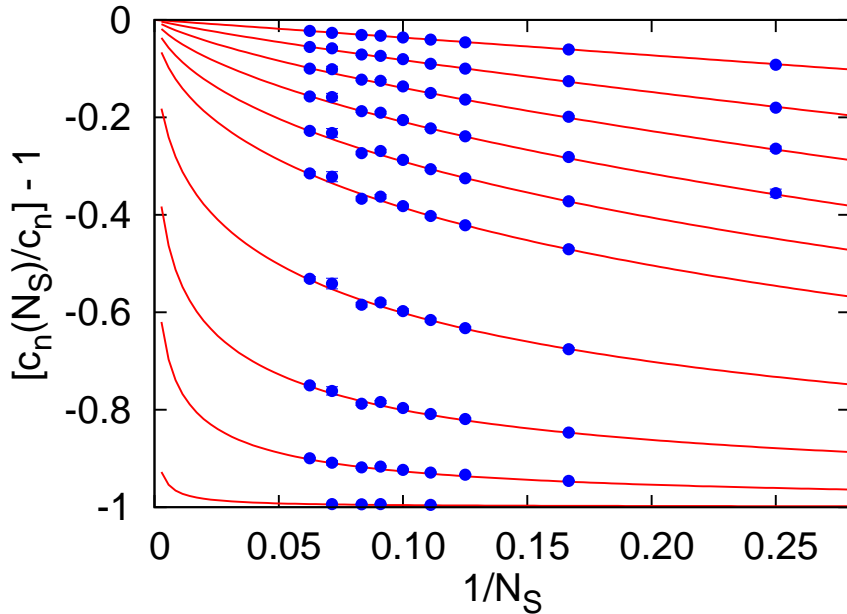


Figure 2. $c_n^{(3,0)}(N_S)/c_n^{(3,0)} - 1$ for $n \in \{0, 1, 2, 3, 4, 5, 7, 9, 11, 15\}$ (top to bottom). For each value of N_S we have plotted the data point with the maximum value of N_T . The curves represent the global fit. $-(1/N_S)f_{0,\text{DLPT}}^{(3,0)}/c_{0,\text{DLPT}}^{(3,0)}$ is shown for $n = 0$. From [11].

For large N_S , we write (using the ‘‘perturbative’’ OPE: $\frac{1}{a} \gg \frac{1}{N_S a} \gg \Lambda_{\text{QCD}}$)

$$\delta m(N_S) = \frac{1}{a} \sum_{n=0}^{\infty} c_n \alpha^{n+1} \left(a^{-1} \right) - \frac{1}{aN_S} \sum_{n=0}^{\infty} f_n \alpha^{n+1} \left((aN_S)^{-1} \right) + \mathcal{O} \left(\frac{1}{N_S^2} \right). \quad (6)$$

We next Taylor expand $\alpha((aN_S)^{-1})$ in powers of $\alpha(a^{-1})$:

$$c_n(N_S) = c_n - \frac{f_n(N_S)}{N_S} + \mathcal{O} \left(\frac{1}{N_S^2} \right), \quad f_n(N_S) = \sum_{i=0}^n f_n^{(i)} \ln^i(N_S), \quad (7)$$

where $f_n^{(0)} = f_n$ and the coefficients $f_n^{(i)}$ for $i > 0$ are determined by f_m with $m < n$ and β_j with $j \leq n-1$.

$$\begin{aligned} f_1(N_S) &= f_1 + f_0 \frac{\beta_0}{2\pi} \ln(N_S), \\ f_2(N_S) &= f_2 + \left[2f_1 \frac{\beta_0}{2\pi} + f_0 \frac{\beta_1}{8\pi^2} \right] \ln(N_S) + f_0 \left(\frac{\beta_0}{2\pi} \right)^2 \ln^2(N_S), \end{aligned}$$

and so on. Eq. (7) gives us the functional form to fit to the lattice data at different volumes. We show how the fits look in Fig. 2.

2.2. Physical interpretation

The second term in Eq. (6) can be interpreted as the interaction of the Polyakov loop with its mirror image. See Fig. 3. This is a reflection of working in a finite volume, which acts as an

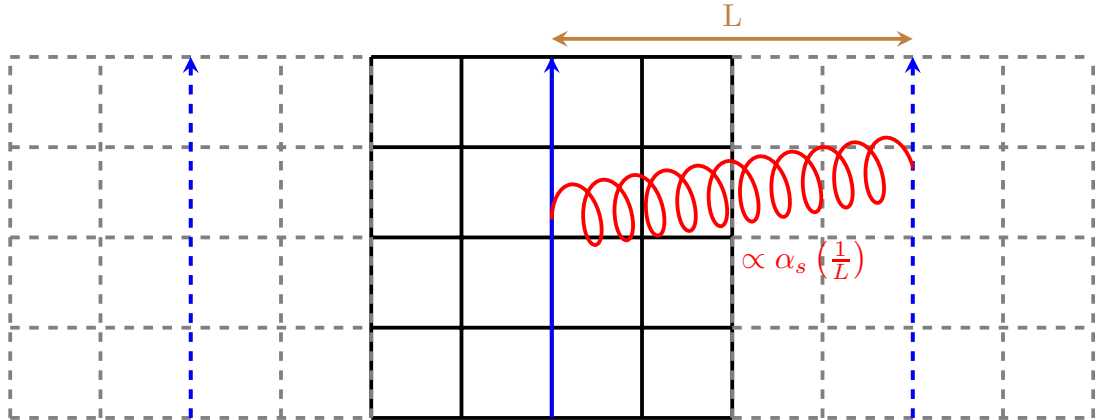


Figure 3. Self-interactions with replicas producing $1/L = 1/(aN_S)$ Coulomb terms.

infrared regulator. Therefore, the result can also be understood in this way, as one can see from a simplified large- β_0 computation:

$$P \propto \int_{1/(aN_S)}^{1/a} dk \alpha(k) \sim \frac{1}{a} \sum_n c_n \alpha^{n+1} (a^{-1}) - \frac{1}{aN_S} \sum_n c_n \alpha^{n+1} ((aN_S)^{-1}),$$

$$c_n \simeq N_m \left(\frac{\beta_0}{2\pi} \right)^n n!, \quad f_n^{(i)}(N_S) \simeq N_m \left(\frac{\beta_0}{2\pi} \right)^n \frac{n!}{i!}. \quad (8)$$

2.3. Comparison with renormalons

Once we have the coefficients c_n from the infinite volume extrapolation, we can compare them with renormalon expectations. The following ratio is a pure prediction from renormalons:

$$\frac{c_n^{(3,\rho)}}{c_{n-1}^{(3,\rho)}} \frac{1}{n} = \frac{c_n^{(8,\rho)}}{c_{n-1}^{(8,\rho)}} \frac{1}{n} = \frac{\beta_0}{2\pi} \left\{ 1 + \frac{b}{n} - \frac{bs_1}{n^2} + \frac{1}{n^3} [b^2 s_1^2 + b(b-1)(s_1 - 2s_2)] + \mathcal{O}\left(\frac{1}{n^4}\right) \right\},$$

which we compare in Fig. 4 with the analogous ratio using the c_n obtained from the fits. We observe a nice agreement for large n .

We can also determine the normalization of the renormalons using the following equalities:

$$c_n^{fitted} = N_m \left(\frac{\beta_0}{2\pi} \right)^n \frac{\Gamma(n+1+b)}{\Gamma(1+b)} \left(1 + \frac{b}{(n+b)} c_1 + \frac{b(b-1)}{(n+b)(n+b-1)} c_2 + \dots \right),$$

$$f_n^{fitted} = N_m \left(\frac{\beta_0}{2\pi} \right)^n \frac{\Gamma(n+1+b)}{\Gamma(1+b)} \left(1 + \frac{b}{(n+b)} c_1 + \frac{b(b-1)}{(n+b)(n+b-1)} c_2 + \dots \right).$$

This is shown in Fig. 5.

Out of these results, we can see that the ambiguity of the pole mass, associated to the minimal term, is of order Λ_{QCD} , as stated in Eq. (1), see Fig. 6.

3. CONCLUSIONS

There was already rather appealing evidence for the existence of renormalons in heavy quark physics from $\overline{\text{MS}}$ -like computations: Pole mass, static potential, hybrid potential, and other quantities. What was missing was an indisputable prove of its existence. This is given by the long string of coefficients complying with the renormalon hypothesis. These were obtained

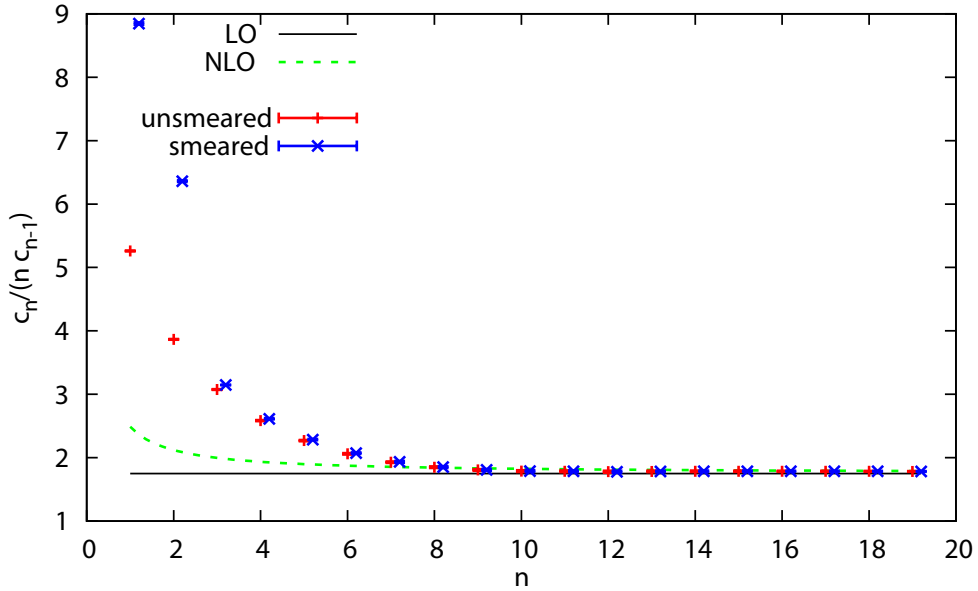


Figure 4. Ratios $c_n/(n c_{n-1})$ of the smeared (blue) and unsmeared (red) triplet static self-energy coefficients c_n in comparison to the theoretical prediction at different orders in the $1/n$ expansion.

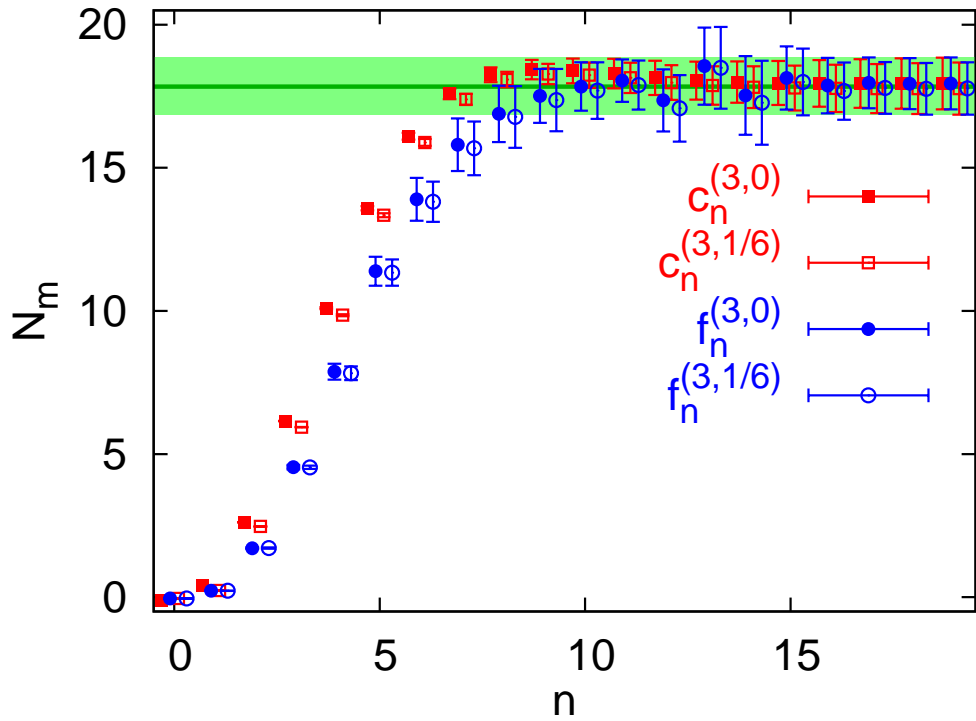


Figure 5. N_m , determined from the coefficients $c_n^{(3,0)}$, $c_n^{(3,1/6)}$, $f_n^{(3,0)}$ and $f_n^{(3,1/6)}$ at NNLO. The horizontal band is our final result: $N_m^{latt} = 17.9 \pm 1.2$. From [12].

in Refs. [10, 11, 12]. For the first time, it was possible to follow the factorial growth of the coefficients over many orders, from around α^8 up to α^{20} .

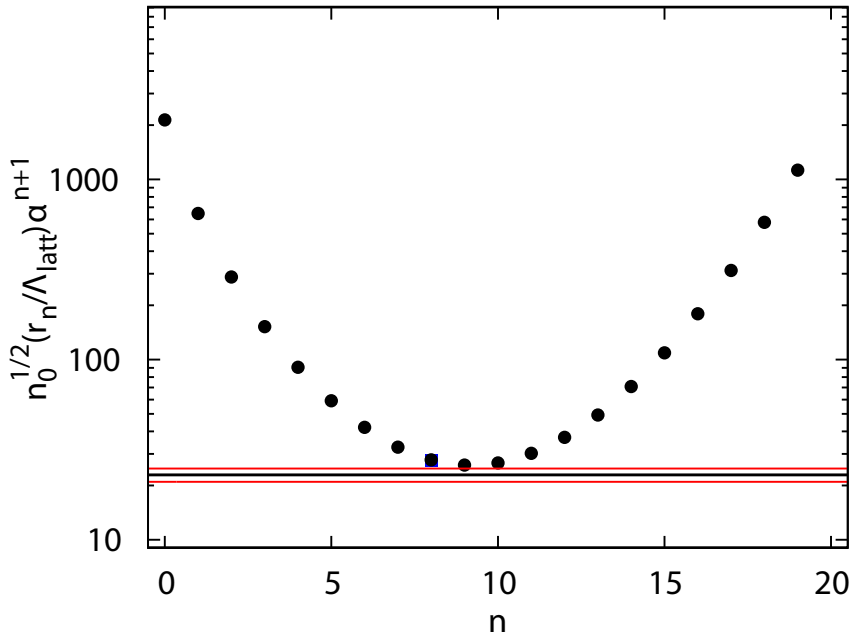


Figure 6. Plot of the asymptotic behavior of $r_n \alpha^{n+1}$ from [11], using $\alpha = 0.057$ and $\nu c_n = r_n$. The minimal term is of order Λ_{QCD} .

We have (numerically) proven, beyond any reasonable doubt (~ 20 standard deviations), the existence of the renormalon in QCD.

3.1. Acknowledgments

I thank G.S. Bali, C. Bauer and C. Torrero for collaboration in the work reviewed here. This work was supported in part by the Spanish Ministry of Science and Innovation (PID2020-112965GB-I00/AEI/10.13039/501100011033), and the grant 2017SGR1069 from the Generalitat de Catalunya. This project has received funding from the European Union's Horizon 2020 research and innovation programme under grant agreement No 824093. IFAE is partially funded by the CERCA program of the Generalitat de Catalunya.

References

- [1] F. J. Dyson, Phys. Rev. **85** (1952) 631.
- [2] G. 't Hooft, in *Proc. Int. School: The whys of subnuclear physics*, Erice 1977, ed. A. Zichichi (Plenum, New York, 1978).
- [3] M. Beneke, Phys. Rept. **317** (1999) 1.
- [4] F. David, Nucl. Phys. B **209** (1982) 433.
- [5] I. M. Suslov, Zh. Eksp. Teor. Fiz. **127** (2005) 1350.
- [6] V. Zakharov, Nucl. Phys. Proc. Suppl. **207** (2010) 306.
- [7] F. Di Renzo, G. Marchesini, P. Marenzoni and E. Onofri, Nucl. Phys. B Proc. Suppl. **34** (1994) 795.
- [8] F. Di Renzo, E. Onofri, G. Marchesini and P. Marenzoni, Nucl. Phys. **B426**, 675 (1994) [arXiv:hep-lat/9405019].
- [9] F. Di Renzo and L. Scorzato, J. High Energy Phys. **0410**, 073 (2004) [arXiv:hep-lat/0410010].
- [10] C. Bauer, G. S. Bali and A. Pineda, Phys. Rev. Lett. **108**, 242002 (2012) [arXiv:1111.3946 [hep-ph]].
- [11] G. S. Bali, C. Bauer, A. Pineda and C. Torrero, Phys. Rev. D **87**, 094517 (2013) [arXiv:1303.3279 [hep-lat]].
- [12] G. S. Bali, C. Bauer and A. Pineda, Proc. Sci. **LATTICE 2013** (2014) 371 [arXiv:1311.0114 [hep-lat]].
- [13] M. Beneke, Phys. Lett. B **344**, 341-347 (1995) [arXiv:hep-ph/9408380 [hep-ph]].
- [14] A. Pineda, JHEP **06**, 022 (2001) [arXiv:hep-ph/0105008 [hep-ph]].
- [15] A. Pineda, PoS **LAT2005**, 227 (2006) [arXiv:hep-lat/0509022 [hep-lat]].